First Observation of the Polytype Phenomenon of Layer Stacking Structure in a Side-Chain-Type Ferroelectric Liquid-Crystalline Polymer

Kohji Tashiro,* Jian-an Hou, and Masamichi Kobayashi

Department of Macromolecular Science, Faculty of Science, Osaka University, Toyonaka, Osaka 560, Japan

Received November 8, 1993; Revised Manuscript Received February 24, 1994®

ABSTRACT: A polytype phenomenon, i.e., a polymorph of layer stacking structure, has been discovered for a side-chain-type ferroelectric liquid-crystalline polymer. The samples cooled from the isotropic state to room temperature at only slightly different rates (0.2 and 0.1 °C/min, for example) showed quite different X-ray diffraction patterns at low Bragg angle, from which the repeating period of layers constructed by mesogenic side groups was evaluated as 68.4 Å for the S1 phase obtained at the cooling rate 0.2 °C/min and 136.8 Å for the S2 phase at 0.1 °C/min. The wide-angle X-ray diffraction and infrared/Raman spectral data were almost the same between these two samples, indicating they take essentially the same inner-layer packing structure. That is, these two samples are different only in their layer stacking structure, i.e., a phenomenon of polytype. The S1 and S2 phases are speculated to be single- and double-layered structures, respectively, where the one layer or the two layers make a repeating period along the normal to the sample plane. A possibility of ferroelectric and antiferroelectric structures has been discussed for the S1 and S2 phases, respectively. By measuring the temperature dependence of the X-ray diffraction, a complicated phase transition has been found to occur among many types of phase with various repeating periods of layers:

$$\mathrm{S1(68.4\ Å)} \xrightarrow{80\ ^\circ\mathrm{C}} \mathrm{S4(62.8\ Å)\ and/or\ S3(218.4\ Å)} \xrightarrow{90\ ^\circ\mathrm{C}} \mathrm{S_C^*(64.0\ Å)} \xrightarrow{100\text{–}140\ ^\circ\mathrm{C}} \mathrm{S_A(68.8\ Å)} \xrightarrow{155\ ^\circ\mathrm{C}} \mathrm{Ch} \xrightarrow{165\ ^\circ\mathrm{C}} \mathrm{isotropic}$$

where S3 is considered to be a triple-layered phase and S_C^*, S_A, and Ch are smectic C, smectic A, and cholesteric phases, respectively.

Introduction

Because of their characteristic electric properties, ferroelectric liquid-crystalline materials have been widely investigated from both scientific and industrial points of view.[1–8] Among them, in particular, ferroelectric liquid-crystalline polymers (FLCP) with chiral mesogenic groups in the skeletal or side chains are very important due to their potentials in controlling the rate of electric dipole inversion under external electric field, in producing mechanically tough materials, in developing easily accessible materials, etc.[9] In spite of this practical importance, however, molecular-dimensional structural studies have been much limited in number because of the high complexity in aggregation structure of layers and in phase transitions.

In a series of papers concerning ferroelectric liquid-crystalline compounds,[10–15] we have clarified a high sensitivity of layer stacking structure to a slight change in sample preparation conditions such as cooling rate from the isotropic phase, type of solvent, etc. High sensitivity of layer stacking structure is not limited only to the low-molecular-weight liquid-crystalline substances but is expected also for the above-mentioned FLCPs. In fact we have found that a side-chain-type FLCP experiences a drastic change in layer stacking structure when the cooling rate from the isotropic state is varied only slightly from 0.2 to 0.1 °C/min, for example. Detailed structural analysis revealed that these stacking structures differ only in their repeating period, i.e., an occurrence of the polytype phenomenon. This phenomenon itself is frequently observed for various types of layer substances including mica, zinc selenide, *n*-paraffin, *n*-fatty acids, etc.[16,17] But, as described in this paper, the polytype phenomenon has been found for the first time in a side-chain-type FLCP system. In this paper, on the basis of X-ray diffraction and infrared spectroscopic measurements, we will report the thus revealed polytype phenomenon and also the characteristic phase transitions which occur during heating or cooling of the FLCP sample.

® Abstract published in *Advance ACS Abstracts*, June 1, 1994.

Experimental Section

Preparation of Samples. The samples used in this study are the FLCP with the following chemical structure (**P1**) and its monomer (**M1**): the latter was used for comparing the transitional behavior with that of the FLCP. These samples were supplied

M1

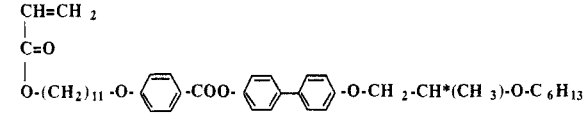

P1

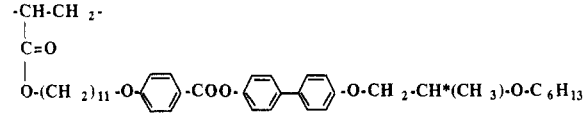

by Canon Ltd., Japan. Details of the synthesis of these materials are described in ref 18. The molecular weight of **P1** is evaluated as M_w = 59 500 and M_n = 26 100.[18] The powder sample packed into a DSC pan was heated up to the isotropic state and then cooled down to room temperature at a well-controlled constant rate. The sample attached on an aluminum base was cut out from the pan and was mounted in the X-ray beam. In some cases the sample was pasted on a thin KBr single-crystal plate and set into a DSC pan: the sample without any metal base could be easily obtained by washing away the KBr substrate with water.

Measurements. The X-ray diffraction patterns of the thus prepared samples were measured by using a Rigaku ROC diffractometer with graphite-monochromatized Cu Kα radiation (λ = 1.5418 Å). The temperature dependence of the X-ray diffraction was measured by using a heater installed at the center of the goniometer in the range of room temperature to ca. 200 °C. The X-ray photograph was taken at room temperature using a flat camera with a sample-to-film distance of 10–15 cm and also

0024-9297/94/2227-3912$04.50/0

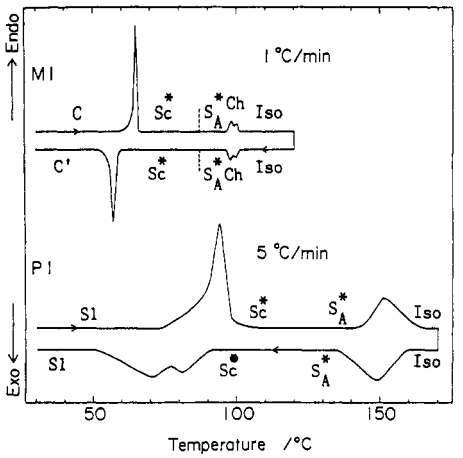

Figure 1. DSC thermograms of **M1** and **P1**.

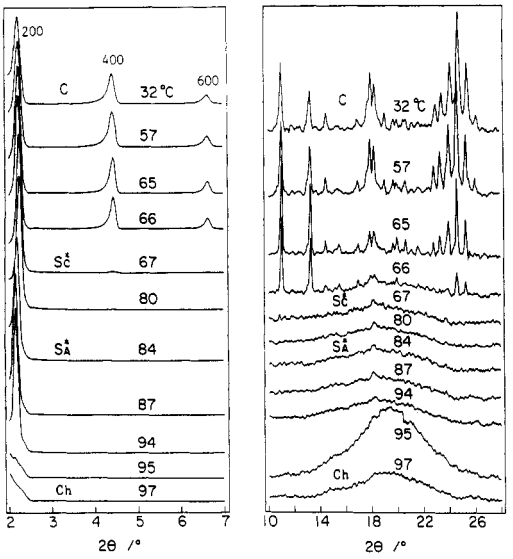

Figure 2. Temperature dependence of the X-ray diffraction pattern of **M1** (heating process).

using an imaging plate system (MacScience Co. Ltd., Japan; DIP100).

The infrared spectra at various temperatures were measured for the KBr disk samples using a Japan Spectroscopic Co. FT-IR 8300 infrared spectrometer.

The DSC thermograms were measured at a heating or cooling rate of 1–5 °C/min using a Seiko DSC20 differential scanning calorimeter.

Results and Discussion

Phase Transition in M1. Before stating the characteristic features of the **P1** sample, the phase transition behavior of **M1** is investigated in this section. Figure 1a shows the DSC thermograms taken for the **M1** sample (the initial **M1** sample was obtained by precipitation from the benzene solution). **M1** shows several sharp endothermic (heating) and exothermic (cooling) peaks. In order to assign the phases in each temperature region, optical microscopic observation and X-ray diffraction measurements were made at various temperatures. In Figure 2 is shown the temperature dependence of the X-ray diffraction pattern measured for the **M1** powder sample (the values 200, 400, and so on indicated in this figure denote the X-ray reflection indices). Referring to the optical microscopic observation, the phases could be assigned to crystal (C), smectic C (S_C*), smectic A (S_A*), cholesteric (Ch), and isotropic (Iso) phases as drawn in the following transition scheme.

$$\begin{matrix} \text{C(40.0 Å)} \overset{67\,^\circ\text{C}}{\underset{50\,^\circ\text{C}}{\rightleftharpoons}} \text{S}_\text{C}^*\text{(39.5 Å)} \overset{89\,^\circ\text{C}}{\underset{83\,^\circ\text{C}}{\rightleftharpoons}} \\ \text{C}'\text{(41.7 Å)} \end{matrix}$$

$$\text{S}_\text{A}^*\text{(41.0 Å)} \overset{99\,^\circ\text{C}}{\underset{96\,^\circ\text{C}}{\rightleftharpoons}} \text{Ch} \overset{101\,^\circ\text{C}}{\underset{98\,^\circ\text{C}}{\rightleftharpoons}} \text{Iso}$$

Here the values in parentheses are the X-ray observed interlayer periods. C′ is the crystal phase obtained in the cooling process from the isotropic state and is different from the initial C phase. In Figures 3 and 4 are shown the temperature dependencies of the infrared and Raman spectra of the **M1** sample, respectively. The infrared bands around 720 cm^{-1}, which are assigned to the CH_2 rocking modes of the trans–zigzag-type methylene sequences, are observed as a doublet in the C phase, indicating the presence of an orthorhombic-type subcell structure of the trans–zigzag methylene chain packing. In the liquid-crystalline (LC) temperature region, the split trans bands decrease in intensity and change into a singlet. Other methylene trans bands around 1460 cm^{-1} decrease also the intensity. The Raman bands are also observed to behave in a way similar to the infrared bands (for example, the methylene trans bands around 2900, 1460, 1100 cm^{-1}, etc.). These spectral changes suggest a transition into the hexagonal (or triclinic) subcell structure consisting of conformationally disordered methylene chains. The infrared and Raman bands due to the benzene and ester groups are also observed to become broader in the LC phases, indicating a disordering in the whole molecular structure and/or a violent molecular motion. A characteristic Raman band is observed around 410 cm^{-1}. In the previous paper[10] we clarified an intimate relationship of this band with the twisted structure of the biphenyl group. A detection of this Raman band in Figure 4 indicates the existence of a twisted biphenyl conformation even in the crystalline phase of the **M1** sample. This band increases its intensity largely in the LC phases, and still in the Iso phase due possibly to an enhanced twist motion around the biphenyl bond.

Polytype Phenomenon in P1. Figure 5 shows the X-ray diffraction patterns measured at room temperature for the **P1** samples prepared in the DSC pan by cooling from the Iso state at the various rates of 5–0.1 °C/min (refer to the Experimental Section). Reflecting a layer stacking structure, a series of intense X-ray reflections can be observed in the small-angle region. For the samples obtained at a rate of 5–0.5 °C/min, the X-ray pattern is essentially the same. The peaks are indexed as 002, 003, 004, 005, and so on, where the c axis is assumed to be perpendicular to the layer plane with a repeating period of ca. 69 Å. (In addition to these intense peaks, there are observed some weak peaks in this small-angle region, as indicated by asterisks, which are considered to come from the other phases as stated below.) The sample obtained at a cooling rate of 0.2 °C/min shows reflections at positions slightly different from those of 0.5 °C/min, but the essential pattern is still the same with the latter. The layer repeating period is estimated as 68.4 Å. Remarkable change is observed in the X-ray diffraction pattern when the cooling rate is changed only by ca. 0.1 °C/min from 0.2 to 0.1 °C/min. That is, the sample cooled at 0.1 °C/min shows the X-ray reflections not only at the same positions with those of the sample cooled at 0.2 °C/min but also at the positions intermediate between these common reflections. If the commonly observed reflections are indexes as l = 2, 3, 4, etc., the additional reflections should be indexed as l = 2.5, 3.5, 4.5, and so on. By doubling the repeating period from 68.4 to 136.8 Å, all the reflections can be

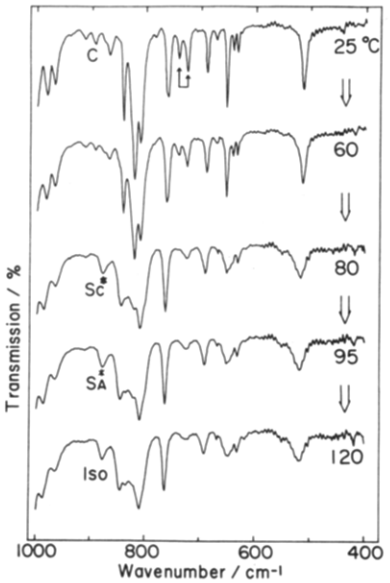

Figure 3. Temperature dependence of Fourier transform infrared spectra of the **M1** sample in the frequency region of 400–1000 cm^{-1} (heating process).

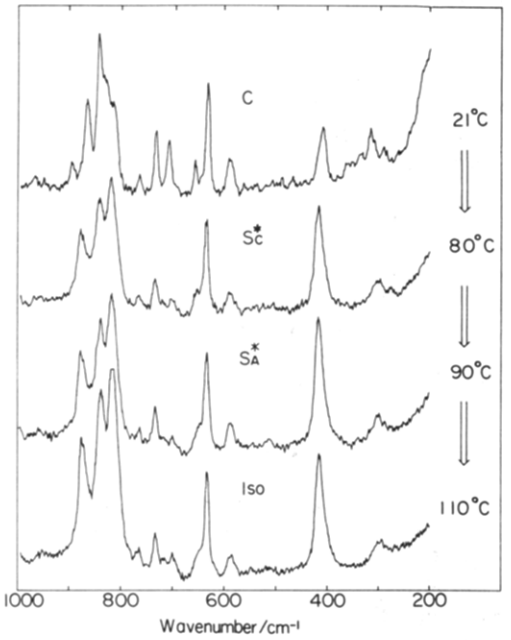

Figure 4. Temperature dependence of Raman spectra of the **M1** sample in the frequency region of 200–1000 cm^{-1} (heating process).

indexed using integers, i.e., $00l$ with $l = 3, 4, 5, 6$, and so on. In Table 1 are listed the indices and interplane distances of the observed reflections.

Figure 6 shows the two-dimensional X-ray patterns measured for the sample prepared at a cooling rate of 0.1 °C/min, where the incident X-ray beam is (a) perpendicular and (b) parallel to the sample plane. In the case of the parallel incidence a highly oriented pattern is obtained, while the perpendicular incidence gives Debye–Sherrer rings. Therefore, the layers are considered to be highly uniaxial around the axis perpendicular to the sample plane. This high degree of orientation is reduced gradually with an increment of the cooling rate as shown in Figure 7, suggesting that the orientational ordering of the stacked layers proceeds very slowly: a rapid cooling results in frozen-in disordered layer stacking. A combination of Figures 5 and 7 clarifies that a slight change in the cooling rate causes not only a change in the degree of layer

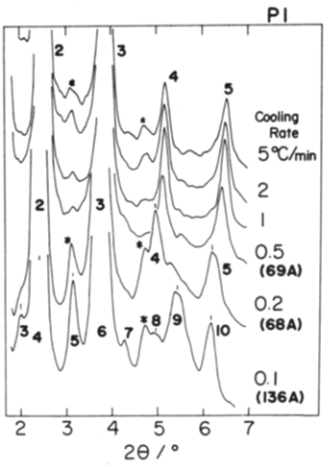

Figure 5. X-ray diffraction patterns of **P1** samples prepared at various cooling rates from the isotropic phase to room temperature. (Asterisks indicate the reflections originating from the not-yet-assigned phases.)

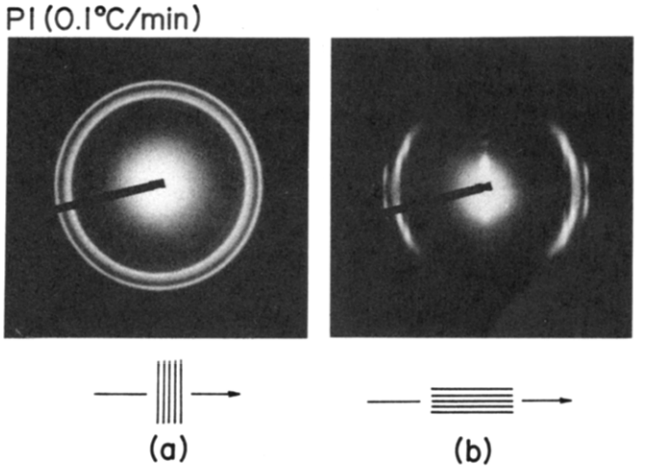

Figure 6. X-ray diagrams taken for the **P1** sample obtained at a cooling rate of 0.1 °C/min. The incident X-ray beam is (a) perpendicular and (b) parallel to the sample plane.

Table 1. Interplanar Spacings and Indices *l* Observed for the X-ray 00*l* Reflections of Various Phases of the P1 Sample

phase	repeating period, Å	interplanar spacings, Å (index *l*)
S1	68.4	68.4 (1), 34.2 (2), 22.5 (3), 17.2 (4), 13.6 (5)
S2	136.8	68.4 (2), 45.6 (3), 34.2 (4), 27.4 (5), 22.5 (6), 19.5 (7), 17.2 (8), 15.2 (9), 13.6 (10)
S3	218.4	35.6 (6), 27.2 (8), 21.8 (10), 18.2 (12), 13.7 (16)
S4	62.8	20.9 (3), 15.7 (4)
S_C*	64.0	32.0 (2), 21.0 (3), 16.0 (4)
S_A	68.8	34.4 (2), 22.9 (3), 17.2 (4)

orientation but also a drastic change in the interlayer spacing.

In Figure 8 shows the X-ray diffraction pattern taken in a wide-angle scattering range. Compared with the remarkable difference of the pattern in the small-angle region (<10°), the reflectional positions in the wide-angle region are almost the same between the two samples cooled at 0.2 and 0.1 °C/min, although the relative intensities are different from each other because of the difference in the degree of orientation (refer to Figures 6 and 7). Therefore, from Figures 5 and 8, we may conclude that the two samples discussed above are different only in the layer repeating period, 68.4 and 136.8 Å, and their intralayer structure is

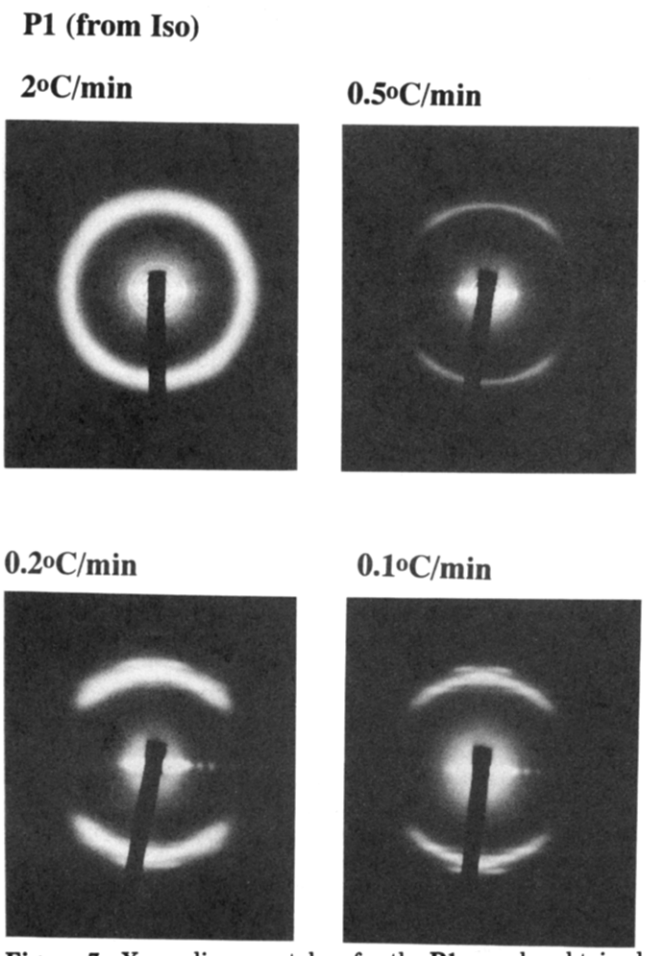

Figure 7. X-ray diagrams taken for the **P1** samples obtained at different cooling rates of 2–0.1 °C/min. The incident X-ray beam is parallel to the sample plane.

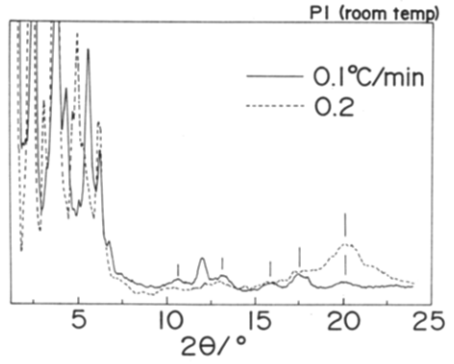

Figure 8. Comparison of X-ray diffraction patterns of the **P1** samples cooled at a rate of 0.1 and 0.2 °C/min.

essentially the same. This type of phenomenon, i.e., a modification of the layer stacking structure, is called polytype. Polytype phenomenon itself is frequently observed for the layer-type substances such as mica, silicon carbide, *n*-paraffin, and *n*-fatty acids, but the present report may be the first example to succeed in finding out the polytypism in the side-chain-type ferroelectric liquid-crystalline polymers. The two types of liquid-crystalline modification found at room temperature are tentatively called S1 and S2. (The reason for the assignment to the liquid-crystalline state comes from the similarity of the infrared spectra with those of the liquid-crystalline phase of the **M1** sample, as discussed in the next section.) **M1** was treated in a way similar to that of **P1**, but no difference was found for the reflections corresponding to the interlayer spacing (ca. 42 Å for the C′ phase), although the

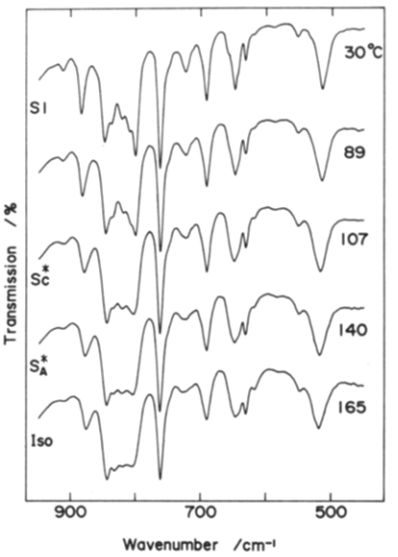

Figure 9. Temperature dependence of infrared spectra of the **P1** sample (S1) in the frequency region of 450–950 cm^{-1} (heating process).

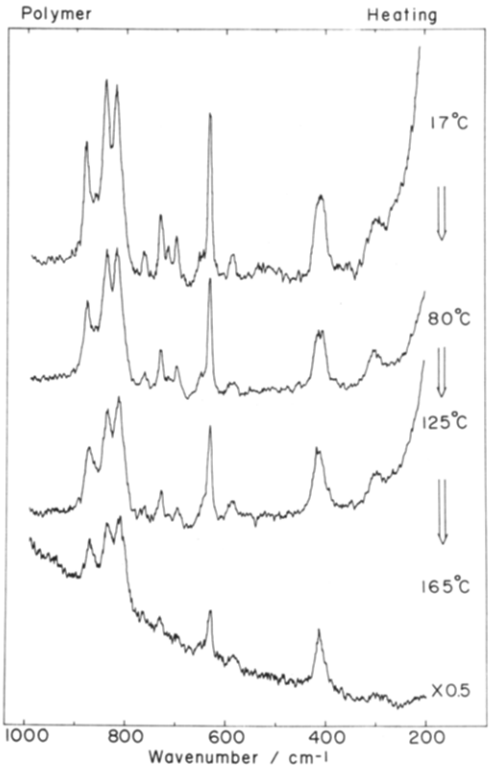

Figure 10. Temperature dependence of Raman spectra of the **P1** sample (S1) in the frequency region of 200–1000 cm^{-1} (heating process).

intralayer structure might be affected somewhat as judged from the slight difference in the wide-angle region. In this way the polytype phenomenon is considered to occur preferentially in the polymer system **P1**. The reason might be correlated with such a situation of the polymer system that the spatial motions of the mesogenic groups are confined by being linked covalently to the skeletal chain and a slight change in a mesogenic group induces a cooperative structural change of the neighboring mesogenic groups in a whole space. A good embodiment of this high cooperativity will be seen in a later section where a complicated phase transitional behavior of the **P1** system is described.

Stacking Structure of Layers in P1. In Figures 9 and 10 are shown the temperature dependencies of infrared

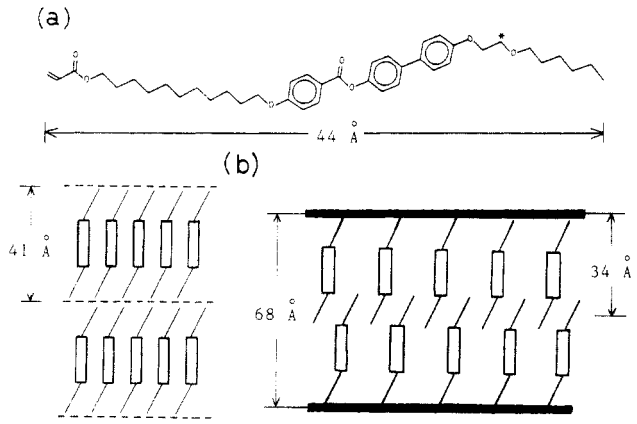

Figure 11. (a) Fully extended **M1** molecular model and (b) layer models of the S_A phase of **M1** (left) and **P1**.

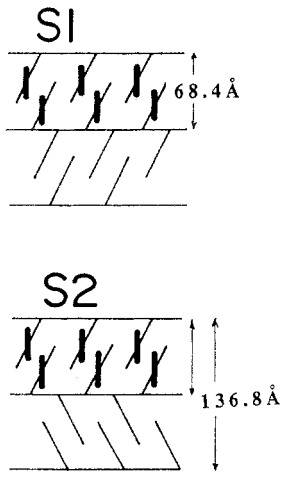

Figure 12. Possible packing structure of S1 and S2 phases.

and Raman spectra of the **P1** sample (S1). By comparing these spectra with those of **M1** in Figures 3 and 4, we may notice that the spectra of **P1** are very similar to those of **M1** in the liquid-crystalline phases. That is to say, the mesogenic groups of **P1** at room temperature (and at high temperatures) are considered to be in a similar conformation with those of the liquid-crystalline state of **M1**. The length of fully extended planar-zigzag chain conformation of **M1** is calculated as ca. 44 Å (see Figure 11a). The layer spacing ca. 41 Å observed for the S_A phase of **M1** is close to this calculated value. A slight difference by ca. 3 Å may come from the conformationally disordered structure of molecules at high temperatures as seen in the infrared and Raman spectra (for example, a twisting in the biphenyl groups, some gauche parts in the methylene sequences, and so on). A similarity in the spectra between **M1** and **P1** suggests that the side chain of **P1** may be assumed basically to have a length close to 41 Å. However, the S_A phase of **P1** takes an interlayer spacing of 68.8 Å. How does it correlate with the value 41 Å? If the mesogenic groups stand vertically in the layer sheets as expected from the conventional structure of the general S_A phase, the side-chain length should be 68.8/2 = 34.4 Å. The value is too short and contradicts the above-mentioned length 41 Å. Rather we might assume that the layers are constructd by an interdigitation of two side-chain groups by ca. 7 Å, as illustrated in Figure 11. By combining this consideration with the experimental result on the interlayer spacing, plausible models of S1 and S2 may be deduced as shown in Figure 12, where the bold line represents a mesogenic group and the thin line represents side-chain groups. Side chains are bonded to the main chain in an *atactic* configurational fashion, but an observation of relatively sharp X-ray equatorial reflections suggests that the packing of the side chains is appreciably regular so as to form a layer of smectic type, even though these side chains stick out of the main chains statistically randomly. Horizontal thin solid lines represent the main chains. The main chains may be assumed to be included in between the layers of side groups as proposed from the neutron scattering experiments on several side-chain-type liquid-crystalline polymers,[19] although we have now no idea of the concrete main-chain conformation. (The detailed three-dimensional packing structure of the side chains is now being calculated by using energy minimization and molecular dynamics techniques, the result of which will be published elsewhere.)

The spacing 68.4 Å observed for S1 and S2 phases is apparently close to that of the S_A phase, 68.8 Å. A slight difference in the spacing might imply a slight tilting of the mesogenic groups as well as some extension of alkyl chain parts, if the thermal mobility of the side groups is depressed at room temperature. (As shown in Figure 6b, an apparent upper and lower splitting of the wide-angle X-ray reflections from the equatorial line might correspond to such a tilting structure of the mesogenic groups although the detailed indexing is not yet made because of a too complicated pattern.) Different from the S_A phase, therefore, we might expect some polarity for the chiral layer structure of the S1 or S2 phase. If such a polarity of one layer is realistic and almost the same in both phases, then it may be expected that S1 is ferroelectric and S2 is antiferroelectric. Watanabe et al. proposed an existence of an anticlined double-layer structure for a main-chain-type LCP.[20] Mensinger et al. speculated about a possibility of antiferro- and ferrielectric structures for various "combined" LCPs where side chains consisting of mesogenic groups are attached in between mesogenic groups in the main chain.[21] An existence of two types of layer stacking structures and a possibility of the ferro- and antiferroelectric structures for one unique LCP, **P1**, may be the first case as already pointed out. Of course, such a speculation should be checked experimentally by measuring, for example, a D–E hysteresis loop where D and E are electric displacement and electric field strength, respectively.[22]

As shown in Figure 5, the X-ray 00l reflections with odd l are detected in the S2 sample although the relative intensity is not so high compared with that of the even-numbered reflections. If the layer stacking is repeated regularly and the structural factor of the layer is common, then the odd-numbered reflections should not be observed due to the requirement of space symmetry. The reason why the odd-numbered reflections are observed in Figure 5 might come from the following situations. (1) As shown in Figure 13, the repeating period of the S2 might be doubled from 136.8 to 273.6 Å, i.e., the four layered structure. Then the reflections with l = 2, 3, 4, 5, ... are reindexed as even-numbered ones (l = 4, 6, 8, 10, ...). (2) The structure factors of the two types of layers might be different from each other, and at the same time some irregular replacements of layers might occur in the S2 phase. For example, the S1 layer is introduced in an irregular fashion into the main S2 layer structure, just when the structure factor should become as follows.

For $l = 2n$ $\quad F(00l) = F_2 + [F_2\omega + F_1(1-\omega)] = (1+\omega)F_2 + (1-\omega)F_1 \neq 0$

For $l = 2n+1$ $\quad F(00l) = F_2 - [F_2\omega + F_1(1-\omega)] = (1-\omega)(F_2 - F_1)$

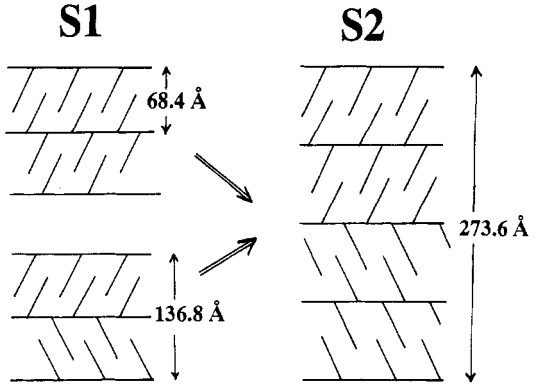

Figure 13. Other S1 and S2 models where the repeating period of layers is doubled from those shown in Figure 12.

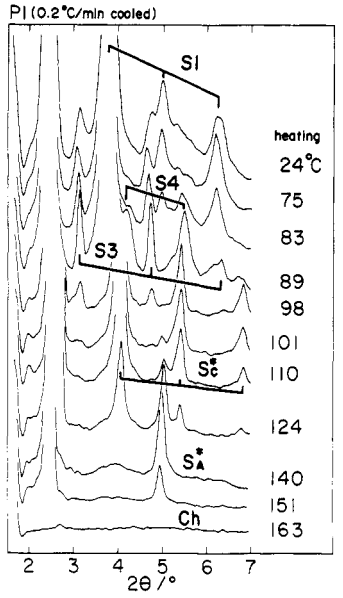

Figure 14. Temperture dependence of X-ray diffraction patterns of the **P1** starting from the S1 state (heating process). Reflections indicated by thick solid lines in this figure are as follows. S1: 22.5, 17.2, 13.6 Å. S4: 20.9, 15.7 Å. S3: 27.2, 18.2, 13.7 Å. S_C*: 21.0, 16.0, 12.8 Å. Refer to Table 1.

where F_1 and F_2 are structure factors of the S1 and S2 layers and ω is the probability of the S1 layer within the S2 layers. If $\omega \neq 1$ and $F_1 \neq F_2$, then both the odd and even reflections should be observed. An assumption of different structure factors F_1 and F_2 may not be impossible if the contribution of the main-chain structure is additionally taken into account in the evaluation of structure factors of the side-chain groups. Of course, such a difference between F_1 and F_2 is not considered to be large, and so the odd-numbered reflections should be weak compared with the even-numbered reflections. In fact, as seen in Figure 5, the actually observed odd-numbered reflections are weak compared with the fully saturated even-numbered reflections in this figure.

Phase Transitions. Figure 14 shows an example of the temperature dependence of X-ray patterns starting from the S1 phase. In Figure 15 is shown the results obtained for the cooling process from the isotropic phase. Analysis of these X-ray data in the heating and cooling processes revealed a complicated transitional scheme shown in Figure 16. In Figure 17 is illustrated the transition between the various phases, where the bold lines represent the mesogenic groups. (In the S_C* phase the mesogenic groups are assumed to be tilted by a certain angle, and in the S_A phase the mesogenic groups are assumed to stand vertically.) The S1 and S2 phases change

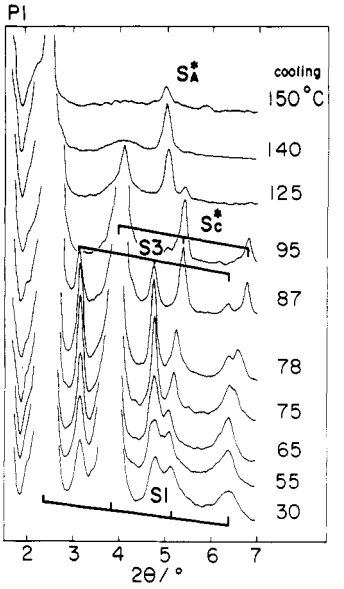

Figure 15. Temperature dependence of X-ray diffraction patterns of **P1** measured during cooling from the isotropic state. Reflections indicated by thick solid lines in this figure are as follows. S_C*: 21.0, 16.0, 12.8 Å. S3: 27.2, 18.2, 13.7 Å. S1: 34.2, 22.5, 17.2, 13.6 Å. Refer to Table 1.

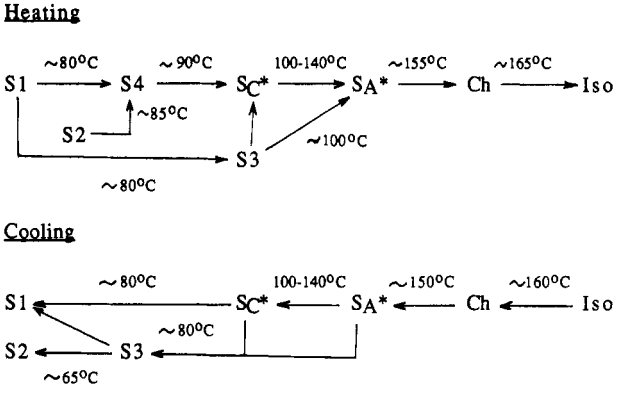

Figure 16. Summarized phase transitional schemes of **P1** in the heating and cooling processes.

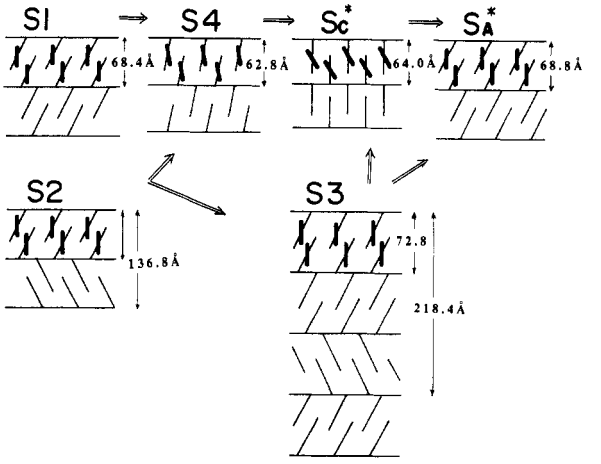

Figure 17. Illustrated layer structural change during the phase transitions among the various phases of **P1**. A bold bar represents a mesogenic group, and a thin line represents an alkyl side chain.

into S_C*, S_A, and cholestric phases *via* new phases having different layer repeating periods (S3 with L = 218 Å and S4 with L = 62.8 Å). The S3 phase appears in the intermediate route from S_C* to S1 (or S2) in the cooling process. The broad endothermic (heating process) and exothermic (cooling process) peaks observed in the DSC thermograms shown in Figure 1 are considered to cor-

respond to these multiple phase transitions. The X-ray reflections observed for this phase are indexed by assuming a triple-layer structure where the three layers make one period. In the cooling process, the layer stacking structure must change from the triple-layer type of S3 to double-layer (S2) or single-layer type (S1) in a complicated manner. Therefore, it may be easily speculated that the sample contains a rather high degree of layer stacking disorder. In the preceding section we pointed out a possibility of stacking disorder in the S1 and S2 phases. The S3 phase is obtained frequently even at room temperature when the cooling rate is not well controlled. This experience may also be well understood from such a viewpoint that the S3 phase may be frozen in the transition to a more stable S1 or S2 phase.

Conclusions

In this paper we reported the first observation of the polytype phenomenon in a side-chain-type FLCP sample. As understood from Figures 5 and 14–16, the **P1** sample is found to experience a variety of phase transitions. At the same time the layer stacking structure is also found to change drastically by a slight change in the cooling (and heating) rate. As already discussed in the previous section, the side chains are connected covalently side by side to the main chain and their mobile spaces are confined to an appreciable extent. Therefore, a slight change in one mesogenic group may induce a cooperative motion of the neighboring side chains and result in a drastically large structural change in the whole layer structure, i.e., a variety of polytype phenomena and a complicated phase transitional behavior. The present **P1** system is also interesting in association with a possibility of ferroelectric behavior. If the arrangement of electric dipoles is varied corresponding to the change in layer stacking structure, then the so-called ferroelectric–antiferroelectric (and ferrielectric) phase transitions might occur in the above transition scheme of Figure 16. Further study is now going on.

Acknowledgment. The authors thank Canon Co. Ltd., Japan, for their kind supply of the **P1** and **M1** samples. This study is supported in part by Grants-in-Aid for Scientific Research from the Ministry of Education, Science, and Culture, Japan (Nos. 03555189 and 04403020).

References and Notes

(1) Meyer, R. B.; Liebert, L.; Strzelecki, L.; Keller, P. *J. Phys. (Paris) Lett.* **1976**, *36*, L–69.
(2) Myer, R. B. *Mol. Cryst. Liq. Cryst.* **1977**, *40*, 33.
(3) Martinot-Lagarde, Ph. *J. Phys. (Paris)* **1977**, *38*, L–17.
(4) Yoshino, K.; Uemoto, T.; Inuishi, Y. *Jpn. J. Appl.* **1977**, *16*, 571.
(5) Hoffmann, J.; Kuczynski, W.; Malecki, J. *Mol. Cryst. Liq. Cryst.* **1978**, *44*, 287.
(6) Clark, N. A.; Lagerwall, S. T. *Appl. Phys. Lett.* **1980**, *36*, 899.
(7) Miyasato, K.; Abe, S.; Takezoe, H.; Fukuda, A.; Kuze, E. *Jpn. J. Appl. Phys.* **1983**, Suppl. 22, 661.
(8) Yoshino, K.; Ozaki, M.; Sakurai, T.; Sakamoto, K.; Honma, M. *Jpn. J. Appl. Phys.* **1984**, Suppl. 23, 175.
(9) *Polymer Liquid Crystals*; Blumstein, A. Ed.; Polymer Science and Technology Series; Plenum Press: New York, 1985.
(10) Tashiro, K.; Hou, J.; Kobayashi, M. *J. Am. Chem. Soc.* **1990**, *112*, 8273.
(11) Hou, J.; Tashiro, K.; Kobayashi, M. *Mol. Cryst. Liq. Cryst.* **1991**, *200*, 145.
(12) Hou, J.; Tashiro, K.; Kobayashi, M. *J. Phys. Chem.* **1991**, *95*, 9561.
(13) Tashiro, K.; Hou, J.; Kobayashi, M. *J. Phys. Chem.* **1992**, *96*, 484.
(14) Hou, J.; Tashiro, K.; Kobayashi, M. *J. Phys. Chem.* **1992**, *96*, 2729.
(15) Tashiro, K.; Hou, J.; Kobayashi, M. *Sen-i Gakkaishi* **1992**, *48*, 410.
(16) Yeomans, J. *Solid State Phys.* **1988**, *41*, 151.
(17) Kobayashi, M.; Kobayashi, T.; Itoh, Y.; Sato, K. *Bull. Mineral.* **1986**, *109*, 171.
(18) Sato, K.; Eguchi, T.; Toshida, Y.; Yoshinaga, K.; Takasu, Y. *Polym. Prepr. Jpn.* **1990**, *39*, 1962, 1965.
(19) Kunchenk, A. B.; Svetogorsky, D. A. *J. Phys. (Paris)* **1986**, *47*, 2015.
(20) Watanabe, J.; Kinoshita, S. *J. Phys. (Paris) II* **1992**, *2*, 1237.
(21) Mensinger, H.; Biswas, A.; Poths, H. *Macromolecules*, **1992**, *25*, 3156.
(22) Takezoe, H.; Lee, J.; Ouchi, Y.; Fukuda, A. *Mol. Cryst. Liq. Cryst.* **1991**, *202*, 85.